Journal of Science and Technology in Civil Engineering NUCE 2020. 14 (2): 116–126

SECOND GRADIENT SUBSTITUTION MODEL FOR HIGH CONTRAST BI-PHASE STRUCTURE

Trinh Duy Khanh[a,*]

[a]*Faculty of Building and Industrial Construction, National of University of Civil Engineering, 55 Giai Phong road, Hai Ba Trung district, Hanoi, Vietnam*

Article history:
Received 24/12/2019, Revised 14/3/2020, Accepted 18/3/2020

Abstract

Lightweight structures with soft inclusion material, such as hollow core slabs, foam sandwich wall, pervious pavement . . . are widely used in construction engineering for sustainable goals. Voids and soft inclusion can be modeled as a very soft material, while the main material is modeled with its original rigidity, which is so much higher than inclusion's one. In consequence, highly contrast bi-phase structure attracts the interests of scientists and engineers. One important demand is how to build a homogeneous equivalent model to replace the multi-phase structure which requires much resources and time to perform structure analysis. Various homogenization schemes have succeeded in establishing a homogeneous substitution model for composite materials which fulfill the scale separation condition (characteristic length of heterogeneity is very small in comparison to structure dimensions). Herein, elastic stiffness matrix of a homogeneous model which replaces a bi-phase material is computed by a higher-order homogenization scheme. A non-homogeneous boundary condition (a polynomial inspired from Taylor series expansion) is used in computation. Homogeneous substitution model constructed from this computation process, can give engineers a fast and effective tool to predict the behavior of bi-phase structure. Instead of a classical Cauchy continuum, second gradient model is selected as a potential candidate for substituting the composite material behavior because of the separation scale (volume ratio of inclusion to matrix phase reaches unit).

Keywords: generalized continuum; second-gradient medium; higher-order homogenization; non-homogeneous boundary conditions; representative volume element.

https://doi.org/10.31814/stce.nuce2020-14(2)-11

1. Introduction

Multi-phase materials are widely used to construct structural members since recent decades. Local mechanical behavior of each phase has impact on global member's one. Therefore, engineers have to take into account all local characters in their simulation. Such analyse requires a lot of computer resources as well as computation time. For this reason, homogenization technique is developed to overcome this challenge by establishment of a homogeneous model which requires much less resources and can give a rapid prediction of global mechanical behavior. This technique has been developed initially in the frame of mechanic and engineering of materials as mentioned in [1, 2] and expanded to structural engineering, for instance [3–5]. In these later works, a homogeneous substitution model are developed to substitute a bridge deck (composed of precast concrete panel), a hollow core slab (whose the void formers are plastic boxes), and brick masonry. These studies concentrate on periodic

*Corresponding author. *E-mail address:* khanhtd@nuce.edu.vn (Khanh, T. D.)

structures, which means the whole structure configuration can be built from translation of unit cell repeatedly in all directions. Some interesting results from these works are presented, but some discussion still remain. In [3], a special boundary condition is developed to transform a 3D periodic bridge deck modeled in detail (so-called micro-mechanical model) to a homogeneous orthotropic thick plate model (so-called macro-mechanical model). In [4], periodic Representative Volume Element (RVE) of hollow core slab is considered. A similar strategy as in [3] is performed. The homogeneous substitution thin shell is finally obtained after the homogenization scheme. Validation of the final substitution model hasn't presented yet. In [5], homogeneous model of Reissner-Midlin orthotropic plate is constructed to substitute a brickwork masonry. The boundary condition is also specific to capture the real behaviour of masonry. Above works show that for different macro-scale structures, boundary condition varies so much. Thus, each homogeneous scheme can be specifically used for one type of structure (voided panels deck, hollow core slab, brick masonry). For other types, new boundary condition development needs to be performed, while in classical homogenization problem, in particular, the case of periodic continuum, boundary condition is stable as described in Section 1. On other side, one can recognize that in above works, structures composed of bi-phased material have been considered (pre-tensioned concrete and mortar phases in [3], reinforced concrete and plastic void formers phases in [4], brick and mortar in [5]). In this paper, a periodic structure composed of two different materials with high contrast mechanical properties is considered. That means the matrix phase is hard and the inclusion one is much softer. Interest of this kind of structure rises because of the increasing use of composite structures with voids or void former in construction engineering such as foam or recycled aggregate concrete, pervious pavement, and hollow core slabs or walls. This research aims at exposing a more general homogenization scheme which can be applied to various types of high contrast bi-phased structures. The essence of this scheme is using a high order polynomial boundary condition, applied on a RVE mechanical problem, to obtain a homogeneous second-gradient continuum. One can notice that all above mentioned structures do not fulfill the scale separation condition which is described in detail in Section 2. The main idea of classical homogenization is recalled here for readers who don't have background of homogenization. Homogenization is a tool to determine the mechanical properties of a homogeneous structure in the macro-scale from its heterogeneous micro-structure in a smaller scale. For this purpose, a mechanical problem, in which a homogeneous boundary condition is applied to a RVE, which has all information of the micro-structure, is established.

$$\begin{cases} \sigma_{ij,j} + f_i & = 0 \\ \varepsilon_{ij} & = \dfrac{1}{2}\left(\dfrac{\partial u_i}{\partial x_j} + \dfrac{\partial u_j}{\partial x_i}\right) \\ \sigma^m_{ij} & = C^m_{ijkl}\varepsilon^m_{kl} \quad \text{on matrix phase} \\ \sigma^i_{ij} & = C^{inl}_{ijkl}\varepsilon^i_{kl} \quad \text{on inclusion phase} \\ & \text{Boundary condition on RVE edges} \end{cases} \tag{1}$$

Boundary conditions in (1) may be a kinematic uniform boundary condition (so called KUBC) or a stress uniform boundary condition (so called SUBC), or a periodic boundary condition which is used in case of periodic structure. They are recalled respectively here for a more clear explanation:

$$\underline{\boldsymbol{u}} = \underset{\sim}{\boldsymbol{E}}^0.\underline{\boldsymbol{x}}\,; \qquad \underset{\sim}{\sigma}.\underline{\boldsymbol{n}} = \underset{\sim}{\boldsymbol{\Sigma}}^0.\underline{\boldsymbol{n}}\,; \qquad \underline{\boldsymbol{u}} = \underset{\sim}{\boldsymbol{E}}^0.\underline{\boldsymbol{x}} + \underline{\boldsymbol{v}} \tag{2}$$

where $\underline{\boldsymbol{a}}$, $\underset{\sim}{\boldsymbol{a}}$ successively denote vector; second-order tensor; $\underline{\boldsymbol{u}}$ denotes displacement vector, $\underline{\boldsymbol{x}}$ denotes position vector of nodes on boundary, $\underline{\boldsymbol{n}}$ denotes normal vector of boundary edges and $\underline{\boldsymbol{v}}$ denotes

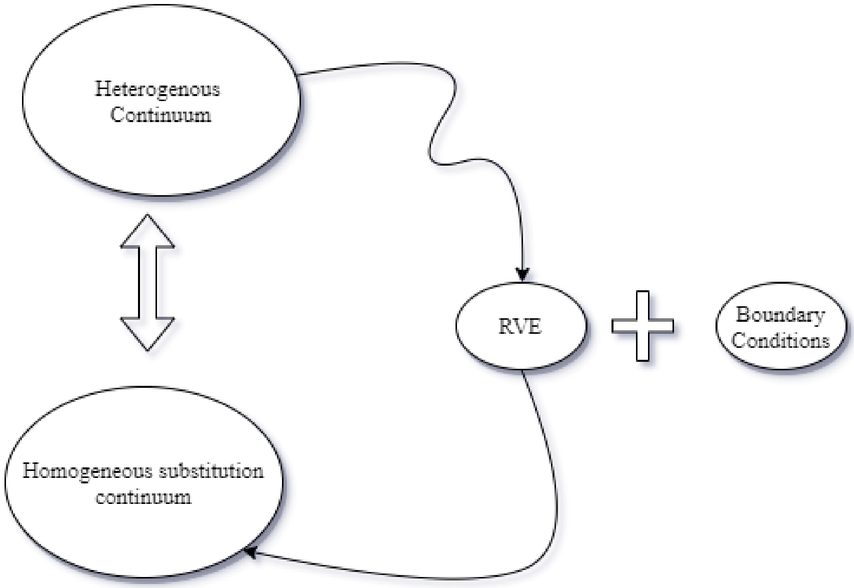

Figure 1. Classical homogenization process

periodic fluctuation of displacement prescribed on the boundary of RVE; $\underset{\sim}{\boldsymbol{E}}^0, \underset{\sim}{\boldsymbol{\Sigma}}^0$ denote respectively the macro scale tensors of deformation and stress. Principle of classical homogenization is illustrated in the Fig. 1. Once the problem (1) is solved, macro scale variables $\underset{\sim}{\boldsymbol{\Sigma}}$, $\underset{\sim}{\boldsymbol{E}}$ of homogeneous substitution structure can be computed as average of corresponding micro scale variables $\underset{\sim}{\boldsymbol{\sigma}}$, $\underset{\sim}{\boldsymbol{\varepsilon}}$ on RVE:

$$\underset{\sim}{\boldsymbol{\Sigma}} = \frac{1}{V}\int_V \underset{\sim}{\boldsymbol{\sigma}}.dV; \qquad \underset{\sim}{\boldsymbol{E}} = \frac{1}{V}\int_V \underset{\sim}{\boldsymbol{\varepsilon}}.dV \tag{3}$$

Based on behavior law of homogeneous equivalent continuum (macro-scale model) as described in Eq. (4).

$$\underset{\sim}{\boldsymbol{\Sigma}} = \underset{\approx}{\boldsymbol{C}}^{eff} : \underset{\sim}{\boldsymbol{E}} \qquad \text{or} \qquad \Sigma_{ij} = C^{eff}_{ijkl}.E_{kl} \tag{4}$$

One can compute the components of C^{eff}_{ijkl} (effective stiffness matrix of macro-scale model) as in (5)

$$\underset{\approx}{\boldsymbol{C}}^{eff} = \begin{bmatrix} \Sigma^*_{11}(E_{11}) & \Sigma^*_{11}(E_{22}) & 0.5\Sigma^*_{11}(E_{12}) \\ \Sigma^*_{22}(E_{11}) & \Sigma^*_{22}(E_{22}) & 0.5\Sigma^*_{22}(E_{12}) \\ \Sigma^*_{12}(E_{11}) & \Sigma^*_{12}(E_{22}) & 0.5\Sigma^*_{12}(E_{12}) \end{bmatrix} \tag{5}$$

with $\Sigma^*_{ij}(E_{k'l'})$ is deduced from problem (1) in the case $E_{\alpha\beta} = \delta_{\alpha'\alpha}\delta_{\beta'\beta}$; with δ_{ij} is Kronecker delta.

2. Generalized continua and higher-order homogenization

2.1. Generalized continua

For structural members used in construction, automobile or marine industry, size of heterogeneity is comparable to overall dimensions. This character does not fulfill scale separation condition of classical homogenization. Mathematical description of latter condition is $l << L^{RVE} << L^{st}$, where l, L^{RVE}, L^{st} are respectively the characteristic length of micro-structure, RVE and macro-structure.

As a consequence, classical homogenization cannot be valid anymore for these structures. As presented above in Section 1, the substitution homogeneous continua are restricted in the framework of Cauchy continuum mechanics with various boundary conditions. For cases of non-scale-separation, the generalized continua rise as hopeful candidates for homogeneous substitution models as in [6–8]. Generalized continua, which can describe the local behavior of micro-structure, are extended from classical Cauchy continuum by adding either new degrees of freedom (DOFs) or high-order derivative of displacement. They have many members for instance, the micromorphic medium (where a micro-deformation second order tensor was added as new DOFs) as in [9], Cosserat or micro-polar medium (where a rotation vector was added to classical DOFs-three translation of displacement) as in [7], or second gradient medium in [10, 11]...where the second derivatives of displacement $u_{i,jk}$ is taken into account beside the classical deformation ε_{ij}. Herein, the second gradient medium is used to construct a substitution homogeneous model for high contrast bi-phase structure. Its equilibrium equations are recalled here:

$$\tau_{ij,j} = 0; \qquad \tau_{ij} = \Sigma_{ij} - m_{ijk,k} \tag{6}$$

where Σ_{ij} and m_{ijk} is classical and hyper stress of second gradient medium. These stress are connected to deformation and second gradient of displacement through the stiffness coefficients in elastic case:

$$\begin{aligned} \Sigma_{ij} &= C_{ijkl} E_{kl} \\ m_{ijk} &= A_{ijkpqr} U_{p,qr} = A_{ijkpqr} K_{pqr} \end{aligned} \tag{7}$$

where $U_{p,qr}$ is the second gradient of displacement, $K_{pqr} = U_{p,qr}$. Hereinafter, Σ_{ij} is used for homogeneous substitution continuum, to avoid confuse with σ_{ij} - stress in micro-mechanical problem. For the same reason, capital U_i is used to distinguished with the micro displacement u_i in the next parts.

2.2. Higher-order homogenization

A question rises in construction of generalized substitution medium is how to connect classical DOFs of Cauchy medium to new DOFs, or new derivatives of generalized ones. New boundary conditions need to be developed from ones in classical homogenization in order to answer this question. For this purpose, polynomial boundary conditions ansatz as shown in Eq. (8) is a good choice. More details about this boundary condition is mentioned in [12]

$$u_i = E_{ij} x_j + \frac{1}{2} D_{ijk} x_j x_k + \frac{1}{3} D_{ijkl} x_j x_k x_l + \frac{1}{4} D_{ijklm} x_j x_k x_l x_m + \dots \tag{8}$$

where i, j, k, l, m take the values from 1 to 3 (three space dimensions). Ones can recognize that this polynomial has the form of Taylor expansion. In [13], a higher-order homogenization scheme was developed with the concept of cluster RVE which is composed of many periodic unit cells. An unit cell has a square shape whose edge dimension is unit (1 mm). The choice of unit system does not change the generality of mechanical problem. Ones can extend problem to larger scale where structural members or construction works exist.

On its boundary edges, two first terms of polynomial boundary condition in Eq. (8) are applied. That means the original boundary condition in Eq. (8) is restricted to:

$$u_i = E^0_{ij} x_j + \frac{1}{2} D_{ijk} x_j x_k \tag{9}$$

From the remote boundary condition on cluster edges, mechanical variables including first and second gradient of displacement as well as elastic energy are computed only on the central cell as in Fig. 2. In this figure, a periodic composite structure is also described with soft round inclusion whose diameter is equal to 0.8 of square edge, covered by a hard matrix material. Both materials are isotropic elastic whose Young modulus and Poisson coefficients are listed in Table 1. That means the same strategy of micro-mechanical problem in (1) is applied again. But this time, problem is posed on the whole cluster, not only on unit cell; with small modification of boundary condition (B.C)).

$$\begin{cases} \sigma_{ij,j} + f_i & = 0 \\ \varepsilon_{ij} & = \dfrac{1}{2}\left(\dfrac{\partial u_i}{\partial x_j} + \dfrac{\partial u_j}{\partial x_i}\right) \\ \sigma^m_{ij} & = C^m_{ijkl}\varepsilon^m_{kl} \quad \text{on matrix phases} \\ \sigma^i_{ij} & = C^{inl}_{ijkl}\varepsilon^i_{kl} \quad \text{on inclusion phases} \\ & \text{second order B.C on cluster edges} \end{cases} \tag{10}$$

It should remember that this homogenization scheme is a scale translation from microscopic (or meso-scopic) classical Cauchy medium to macroscopic second gradient one. Once the mechanical problem on cluster is solved, we found the stress and deformation field $\underset{\sim}{\boldsymbol{\sigma}}, \underset{\sim}{\boldsymbol{\varepsilon}}$ on cluster domain. In the next step, computation is realized on the central unit cell only. Ones consider Hill-Mandel theorem (mentioned in [14]):

$$< \underset{\sim}{\boldsymbol{\sigma}} : \underset{\sim}{\boldsymbol{\varepsilon}} >= \underset{\sim}{\boldsymbol{\Sigma}} : \underset{\sim}{\boldsymbol{E}} + \underset{\approx}{\boldsymbol{M}} \vdots \underset{\approx}{\boldsymbol{K}} = \underset{\sim}{\boldsymbol{E}} : \underset{\approx}{\boldsymbol{C}}^{eff} : \underset{\sim}{\boldsymbol{E}} + \underset{\approx}{\boldsymbol{K}} \vdots \underset{\approx}{\boldsymbol{A}}^{eff} \vdots \underset{\approx}{\boldsymbol{K}} \tag{11}$$

where capital letters $\boldsymbol{\Sigma}, \boldsymbol{M}, \boldsymbol{E}, \boldsymbol{K}$ denote respectively stress, hyper stress, strain, hyper strain in macroscopic medium (second gradient); small letters σ, ε denote stress and strain of microscopic medium (classical Cauchy); $< q >$ denotes $\dfrac{1}{V}\displaystyle\int_V q.dV$ - average of an amount q. Remember that on right hand side of Eq. (11), all variables belong to the substitution second gradient medium, but $\underset{\sim}{\boldsymbol{E}}$ and $\underset{\approx}{\boldsymbol{K}}$ can be computed by average operators always on central unit cell:

$$E_{ij} =< \varepsilon_{ij} >; \qquad K_{ijk} =< u_{i,jk} > \qquad \qquad \text{only on central unit cell} \tag{12}$$

Left-hand side of Eq. (11) is easily computed as cluster problem is solved. It is equal to two times of average of potential energy on central unit cell. Work in [13] showed that cluster problem in Eq. (10) can be divided into two small problems (body load f_i can be ignored for simplicity):

$$\begin{cases} & \text{Problem (a):} \\ \sigma_{ij,j} & = 0 \\ \varepsilon_{ij} & = \dfrac{1}{2}\left(\dfrac{\partial u_i}{\partial x_j} + \dfrac{\partial u_j}{\partial x_i}\right) \\ \sigma^m_{ij} & = C^m_{ijkl}\varepsilon^m_{kl} \quad \text{on matrix} \\ \sigma^i_{ij} & = C^{inl}_{ijkl}\varepsilon^i_{kl} \quad \text{on inclusion} \\ u_i & = E^0_{ij}x_j \quad \text{cluster edges} \end{cases} \qquad \begin{cases} & \text{Problem (b):} \\ \sigma_{ij,j} & = 0 \\ \varepsilon_{ij} & = \dfrac{1}{2}\left(\dfrac{\partial u_i}{\partial x_j} + \dfrac{\partial u_j}{\partial x_i}\right) \\ \sigma^m_{ij} & = C^m_{ijkl}\varepsilon^m_{kl} \quad \text{on matrix} \\ \sigma^i_{ij} & = C^{inl}_{ijkl}\varepsilon^i_{kl} \quad \text{on inclusion} \\ u_i & = \dfrac{1}{2}D_{ijk}.x_j.x_k \quad \text{cluster edges} \end{cases} \tag{13}$$

Problem (a) in Eq. (13) is exactly the same as RVE problem in Eq. (1). It can provide stiffness properties of Cauchy substitution continuum in the same way as in section 1. Problem (b) in Eq. (13) can provide stiffness properties which link strain gradient K_{ijk} to hyper-stress m_{ijk}. Ones can compute

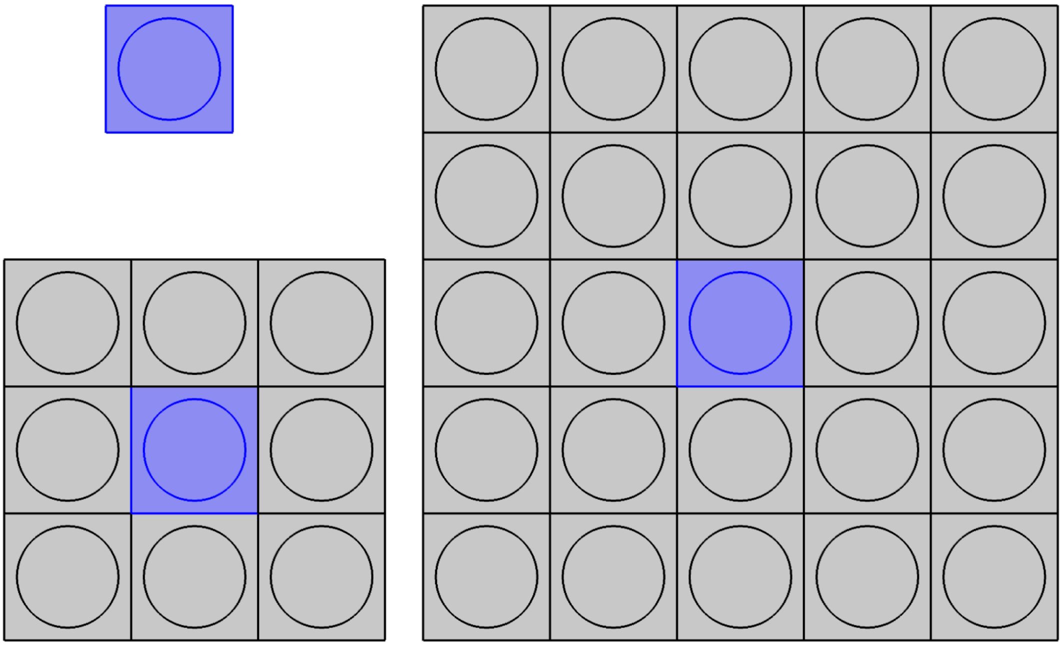

Figure 2. Big clusters of RVE and the central unit cell stress, strain, hyper stress and hyper strain is computed

components A_{ijkpqr} through a similar process as in (5) with small modifications. For explaining in detail the process, we use here $2w$ (with w is the average of potential energy on central unit cell) instead of $< \sigma_{ij}\varepsilon_{ij} >$; $A_{\alpha\beta}K_\alpha K_\beta$ instead of $A_{ijkpqr}.K_{ijk}.K_{pqr}$. Hence, the shortened Hill-Mandell theorem theorem can be rewritten:

$$2w = A_{\alpha\beta}K_\alpha K_\beta \tag{14}$$

Based on Eq. (14), ones can obtain values of A_{ijkpqr} by computing:

$$A_{\alpha\alpha} = 2w(K_{\alpha'}) \qquad \text{with} \qquad K_{\alpha'} = \delta_{\alpha'\alpha} \tag{15}$$

then

$$A_{\alpha\beta} = \frac{1}{2}\left(2w(K_{\alpha'}, K_{\beta'}) - A_{\alpha\alpha} - A_{\beta\beta}\right) \qquad \text{with} \qquad \alpha \neq \beta \tag{16}$$

In Eqs. (15) and (16), $w(K_{\alpha'})$ and $w(K_{\alpha'}, K_{\beta'})$ are solution of problem (b) with $K_{\alpha'} = \delta_{\alpha'\alpha}, K_{\beta'} = \delta_{\beta'\beta}$. Because problem (b) is limited in elastic framework, $K_{\alpha'} = \delta_{\alpha'\alpha}$ can be controlled by changing values of D_{ijk}. It should note that this homogenization scheme did not give an analytical equation but a numerical scheme for determining macroscopic coefficients $\underset{\approx}{\boldsymbol{C}}^{eff}, \underset{\approx}{\boldsymbol{A}}^{eff}$.

3. Validation of substitution model

In the following part, a substitution second gradient model will be constructed in order to replace a highly contrast bi-phase structure. Comparison between homogeneous second gradient model, and heterogeneous Cauchy bi-phase structure will be performed. Two types of RVE (unit cell) in Fig. 3 can be used to represent this periodic structure. To compare the behaviour of two second gradient models (built from RVE type 1 an 2), a double shear problem is considered as described in Fig. 4.

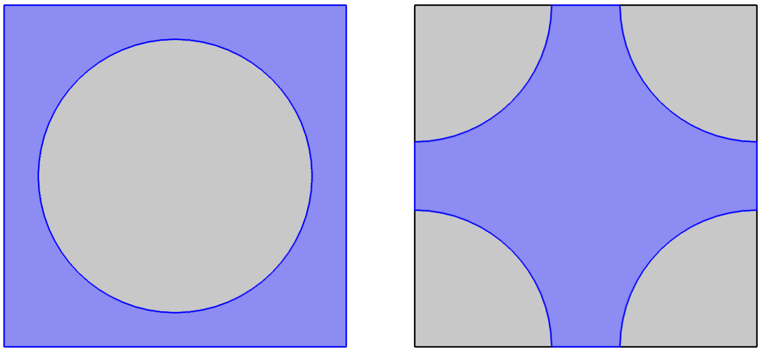

Figure 3. Two types of RVE: Type 1,2 is respectively on the left, right. Bright color represents the soft material, remains are hard one

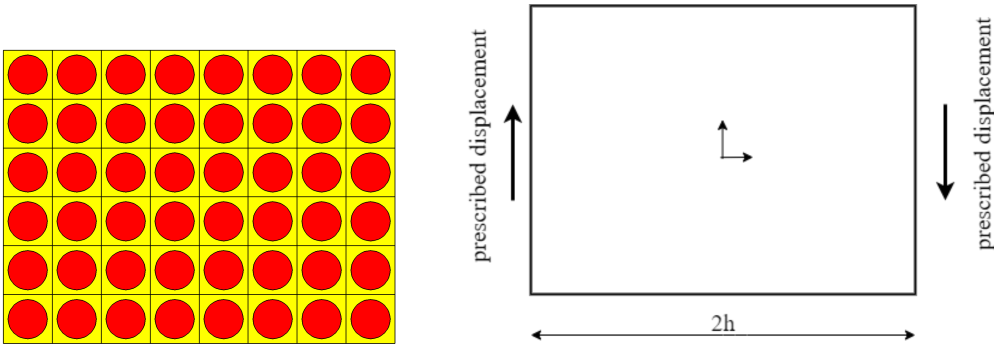

Figure 4. Reference structure (left) where the double shear loading is applied as described in the problem illustration (right)

All computation is realized in the framework of plane stress simulation. Third order elements are used. The reference structure is described on the left of Fig. 4. It is composed of 6×8 unit cells of RVE type 1 in Fig. 3, and supports a double shear loading through two Dirichlet boundary conditions as follow:

$$\begin{aligned} \underline{\boldsymbol{u}} &= \frac{-\delta}{2}\underline{\boldsymbol{e}}_2 \qquad (x = -4 \text{ mm}) \\ \underline{\boldsymbol{u}} &= \frac{\delta}{2}\underline{\boldsymbol{e}}_2 \qquad (x = 4 \text{ mm}) \end{aligned} \tag{17}$$

The substitution homogeneous (second-gradient) structure has the same dimension, and supports the same loading as the reference one. The double shear problem of homogeneous second gradient continuum is described on the right of Fig. 4. Analytical solution of later problem can be found in [12] which was inspired from same loading problem for orthotropic homogeneous second gradient model in [15]. This solution is recalled here for an easy observation:

$$u(x) = \frac{C_1}{\omega^2}\cosh(\omega x) + \frac{C_2}{\omega^2}\sinh(\omega x) + C_3 x + C_4 \tag{18}$$

where $C_1 = C_4 = 0$, $\omega^2 = \dfrac{C_{1212}}{A_{122122}}$ and

$$\begin{aligned} C_2 &= \frac{\delta}{2\left[\dfrac{\sinh(\omega h)}{\omega^2} - \dfrac{h}{\omega}\cosh(\omega h)\right]} \\ C_3 &= \frac{-C_2}{\omega}\cosh(\omega h) \end{aligned} \tag{19}$$

with $2h$ is length of structure along horizontal direction as in Fig. 4; h takes the value of 4 mm in this case; origin of coordinate system coincide with the rectangular centre. Ones can see that in this double shear problem, only shear modulus C_{1212} and A_{122122} influences the result. For the brief of paper, only two later modulus will be presented.

Section 2 provides a homogenization scheme that will be used in this section to obtain the effective properties of second gradient substitution model for a highly contrast bi-phase structure as in Fig. 4. In this paper, the prescribed displacement magnitude $\delta = 0.5$ is taken. The reference structure is composed of two isotropic materials whose mechanical properties are listed in the Table 1.

Table 1. Mechanical properties of isotropic materials in bi-phase structure

Isotropic Properties	Materials	
	Hard phase	Soft phase
Young modulus (MPa)	200000	5
Poisson coefficient	0.3	0.3

Effective properties of substitution model are computed according to cluster problem described in Eq. (13); based on two types of RVE in Fig. 3. These properties are listed in the Table 2. FEM analysis of two problems are carried out: one with the bi-phase (reference) structure, other with the homogeneous Cauchy one whose C^e_{ijkl} is computed from RVE type 1; both structures support double shear loading. Deformed shape as well as the shear stress of these two simulations are performed in Fig. 5 where ones can see the non-smooth displacement of reference structure, in particular on horizontal edges, where reference displacement has the wave form while the corresponding displacement of homogeneous Cauchy model is linear. The zoom-in figure of liberal edges of reference structure is shown in Fig. 6. In particular, shear stress field is largely different between two analysis.

Table 2. Mechanical properties of substitution model

Types of RVE	Effective properties	
	Cauchy homogeneous C_{1212} (MPa)	Second gradient homogeneous A_{122122} (MPa.mm^2)
RVE type 1	7471	−4879300
RVE type 2	7480	1556900

Above displacement fields are compared to corresponding displacement of substitution models in Fig. 7. Their effective properties, shown in Table 2, are computed respectively from RVE type 1

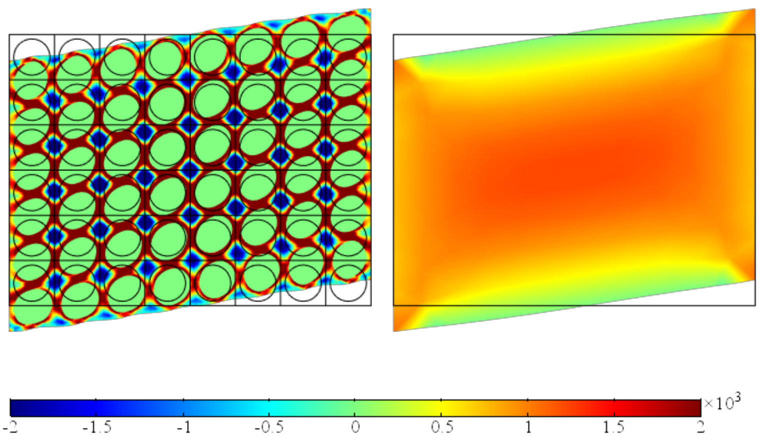

Figure 5. Deformed shape and shear stress (in MPa) of bi-phase structure (on the left) and Cauchy substitution model (on the right)

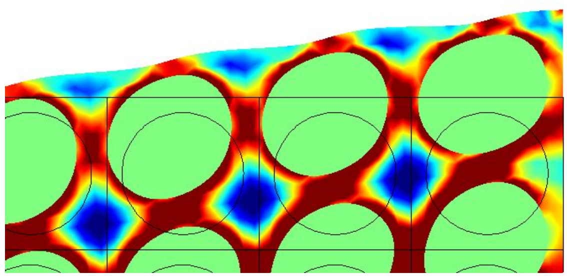

Figure 6. Zoom in on the boundary edges of reference structure

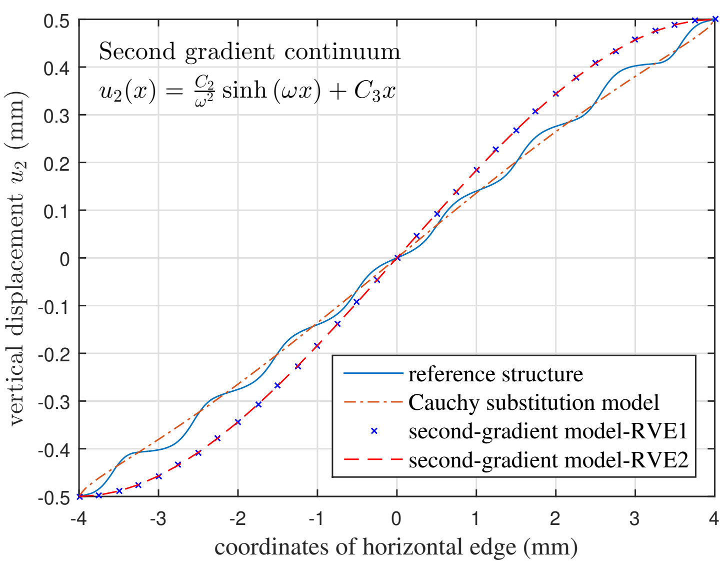

Figure 7. Comparison of displacement on liberal edge of bi-phase (reference) structure, homogeneous Cauchy model, and two substitution (homogeneous second gradient) models (built from RVE 1 and RVE 2)

and RVE type 2. Shape of displacement profile provided by Cauchy substitution model, is very different from one of reference structure. Although closer approximation of Cauchy displacement profile to reference one is detected in Fig. 7, in comparison to second gradient one, it cannot be used for engineering design; because safety conservation always be required in practical standards. Using of Cauchy model can lead to underestimation of structure displacement that is unacceptable. On the contrary, displacement profile provided by second gradient model can cover one of reference structure and give better imagination of actual displacement by means of its curved form.

An extended study should be realized in the future, in order to investigate the stress and strain field in second-gradient model. This can be carried out by using either a special element implemented in the FEM software, or a general solver of partial differential equation (PDE) solver that can solve weak form directly. For the second possibility, COMSOL software is a good choice; and works in [16], where a weak form of second gradient continuum is constructed for implementing FEM elements in Code_Aster software, rise as candidate for next study.

4. Summary and conclusions

Works and results in this paper are summarized:

- Two RVEs of a bi-phase material are considered to compute effective properties of substitution (second gradient) models by a higher-order homogenization scheme (described in Section 2).

- Displacement of these two substitution models, who both are under action of double shear loading, are formulated in Eq. (18).

- A double shear loading problem is computed by COMSOL software on reference structure and homogeneous Cauchy model derived from classical homogenization in Section 1.

- Displacement from above four models are compared in the Fig. 7.

Ones can see that the Cauchy substitution model cannot describe the reference displacement (linear form versus wave one). Displacement of second gradient substitution models, which has the hyperbolic sine form, describe better the reference one. At least, they can be considered as the bound of displacement field, and can be used to predict the displacement of reference structure with a reduced coefficient, which can be object of other studies.

Both substitution (second gradient) continua give a great consistency, while the second gradient properties (in the Table 2) are considerably different. It shows that second-gradient properties have limited contribution in the value of displacement. It is not the case in the form of displacement.

Prediction quality of substitution model can be improved in future study. Other generalized models (Cosserat or micromorphic models) can be used on the one hand, homogenization can be improved on the other hand, thanks to recent discoveries, for example in [17, 18].

References

[1] Sanchez-Palencia, E., Zaoui, A. C. (1987). *Homogenization techniques for composite media: Lectures delivered at the CISM International Center for Mechanical Sciences, Udine, Italy, July 1-5, 1985.* Springer-Verlag.

[2] Nguyen, H.-P., Le, V.-C., Nguyen, T.-K. (2019). Determination of the effective properties of random orientation polycrystals using homogenization method. *Journal of Science and Technology in Civil Engineering (STCE) - NUCE*, 13(4V):129–138. (in Vietnamese).

[3] Attanayake, U., Akbay, Z., Aktan, H. (2011). Three-dimensional modeling and analyses of orthotropic bridge decks using representative volume element. *Practice Periodical on Structural Design and Construction*, 16(4).

[4] Duong, N. T. (2018). Stiffness modified parameters for thin shell model in structural design using ETABS software. *Journal of Building Science and Technology*, 3/2018:8.

[5] Cecchi, A., Sab, K. (2007). A homogenized Reissner–Mindlin model for orthotropic periodic plates: Application to brickwork panels. *International Journal of Solids and Structures*, 44(18):6055–6079.

[6] Trinh, D. K., Janicke, R., Auffray, N., Diebels, S., Forest, S. (2012). Evaluation of generalized continuum substitution models for heterogeneous materials. *International Journal for Multiscale Computational Engineering*, 10(6):527–549.

[7] Forest, S. (1998). Mechanics of generalized continua: construction by homogenizaton. *J. Phys. IV France*, 08(PR4):39–48.

[8] Sab, K. (2009). Overall ultimate yield strength of a quasi-periodic masonry. *Comptes Rendus Mécanique*, 337(8):603–609.

[9] Forest, S. (2009). Micromorphic approach for gradient elasticity, viscoplasticity, and damage. *Journal of Engineering Mechanics*, 135(3):117–131.

[10] Auffray, N., Bouchet, R., Bréchet, Y. (2009). Derivation of anisotropic matrix for bi-dimensional strain-gradient elasticity behavior. *International Journal of Solids and Structures*, 46(2):440–454.

[11] Auffray, N., Le Quang, H., He, Q. C. (2013). Matrix representations for 3D strain-gradient elasticity. *Journal of the Mechanics and Physics of Solids*, 61(5):1202–1223.

[12] Trinh, D. K. (2011). Méthode d'homogénéisation d'ordre supérieur pour les matériaux architecturés. Phd thesis in french, École Nationale Supérieure des Mines de Paris.

[13] Forest, S., Trinh, D. K. (2011). Generalized continua and non-homogeneous boundary conditions in homogenisation methods. *ZAMM - Journal of Applied Mathematics and Mechanics / Zeitschrift für Angewandte Mathematik und Mechanik*, 91(2):90–109.

[14] Bornert, M., Bretheau, T., Gilormini, P. (2001). *Homogénéisation en mécanique des matériaux. . 1, 1*. Hermès Science publications, Paris.

[15] Bacigalupo, A., Gambarotta, L. (2010). Second-order computational homogenization of heterogeneous materials with periodic microstructure. *ZAMM - Journal of Applied Mathematics and Mechanics / Zeitschrift für Angewandte Mathematik und Mechanik*, 90(10-11):796–811.

[16] Chambon, R., Caillerie, D., Matsuchima, T. (2001). Plastic continuum with microstructure, local second gradient theories for geomaterials: localization studies. *International Journal of Solids and Structures*, 38 (46):8503–8527.

[17] Barboura, S., Li, J. (2018). Establishment of strain gradient constitutive relations by using asymptotic analysis and the finite element method for complex periodic microstructures. *International Journal of Solids and Structures*, 136-137:60–76.

[18] Yvonnet, J., Auffray, N., Monchiet, V. (2020). Computational second-order homogenization of materials with effective anisotropic strain-gradient behavior. *International Journal of Solids and Structures*, (191-192):434–448.